

COANNIHILATION EFFECTS IN SUPERGRAVITY AND D-BRANE MODELS

R. Arnowitt, B. Dutta and Y. Santoso

*Center For Theoretical Physics, Department of Physics, Texas A&M University, College Station
TX 77843-4242*

(February, 2001)

Abstract

Coannihilation effects in neutralino relic density calculations are examined for a full range of supersymmetry parameters including large $\tan\beta$ and large A_0 for stau, chargino, stop and sbottom coannihilation with the neutralino. Supergravity models possessing grand unification with universal soft breaking (mSUGRA), models with nonuniversal soft breaking in the Higgs and third generation sparticles, and D-brane models with nonuniversal gaugino masses were analysed. Unlike low $\tan\beta$ where m_0 is generally small, stau coannihilation corridors with high $\tan\beta$ are highly sensitive to A_0 , and large A_0 allows m_0 to become as large as 1TeV. Nonuniversal soft breaking models at high $\tan\beta$ also allow the opening of a new annihilation channel through the s-channel Z pole with acceptable relic density, allowing a new wide band in the $m_0 - m_{1/2}$ plane with $m_{1/2} \gtrsim 400$ GeV and m_0 rising to 1 TeV. The D-brane models considered possess stau coannihilations regions similar to mSUGRA, as well as small regions of chargino coannihilation. Neutralino-proton cross sections are analysed for all models and it is found that future detectors for halo wimps will be able to scan essentially the full parameter space with $m_{1/2} < 1$ TeV except for a region with $\mu < 0$ where accidental cancellations occur when $5 \lesssim \tan\beta \lesssim 30$. Analytic explanations of much of the above phenomena are given. The above analyses include current LEP bounds on the Higgs mass, large $\tan\beta$ NLO correction to the $b \rightarrow s\gamma$ decay, and large $\tan\beta$ SUSY corrections to the b and τ masses.

I. INTRODUCTION

Supersymmetry (SUSY) models with R-parity invariance offers a leading candidate for the dark matter observed in the universe at large and locally in the Milky Way galaxy. Thus in models of this type, the lightest neutralino, $\tilde{\chi}_1^0$, is generally the lightest supersymmetric particle (LSP) and hence is absolutely stable. The observed dark matter is then the relic neutralinos left over after the Big Bang. SUSY models are predictive since they can calculate simultaneously the amount of relic density expected, Milky Way detection signals and the production cross sections at accelerators. Thus cosmological, astronomical and accelerator constraints simultaneously constrain the SUSY parameter space.

The procedure for calculating the relic density of neutralinos is well known. (For a review, see [1].) Over the past decade, a number of refinements of the analysis needed to get accurate answers have been included. Thus the treatment of threshold and s-channel resonances in the annihilation cross section in the early universe was discussed in [2–4]. In calculating the relic density, in most of the parameter space it is sufficient to use the two body neutralino annihilation cross section, since the effects of heavier particles are suppressed by the Boltzman factor. However, in special situations, the next to lightest supersymmetric particle (NLSP) may become nearly degenerate with the LSP, and the coupled annihilation channels of LSP-LSP, NLSP-LSP, NLSP-NLSP must be simultaneously considered [2]. This phenomena of coannihilation was considered within the framework of the minimal supersymmetric model (MSSM) in [5] for the situation when the lightest chargino, $\tilde{\chi}_1^\pm$, becomes nearly degenerate with the $\tilde{\chi}_1^0$. In this paper we consider supergravity (SUGRA) models with grand unification of the gauge coupling constants and soft SUSY breaking at the GUT scale $M_G \cong 2 \times 10^{16}$ GeV. The low energy properties of the theory is thus obtained by running the renormalization group equations (RGE) from M_G to the electroweak scale, where SUSY breaking at M_G triggers $SU(2)_L \times U(1)_Y$ breaking at the electroweak scale. Aside from being in accord with the LEP data implying grand unification, radiative breaking of $SU(2)_L \times U(1)_Y$ greatly enhances the predictiveness of the theory as it reduces the number of SUSY parameters, and one finds generally for such models that the $\tilde{\chi}_1^0$ is mostly Bino, and the $\tilde{\chi}_1^\pm$ is mostly Wino (when the soft breaking masses are less than 1 TeV). Then the $\tilde{\chi}_1^0$ and $\tilde{\chi}_1^\pm$ do not become nearly degenerate and this type of coannihilation does not generally take place. (An exception for a class of D-brane models is discussed below.)

More recently it was pointed out that in SUGRA models, the sleptons (particularly the lightest stau, $\tilde{\tau}_1$) can become nearly degenerate with the $\tilde{\chi}_1^0$ leading to a new type of coannihilation, and this was explored for low and intermediate values of $\tan\beta = \langle H_2 \rangle / \langle H_1 \rangle$ [6,7]. (Here $H_{2,1}$ give rise to (u,d) quark masses). In this paper we examine this effect for the full range of $\tan\beta$, i.e. $2 < \tan\beta < 50$ [8]. Further, in addition to $\tilde{\tau}_1 - \tilde{\chi}_1^0$ coannihilation, we find the possibility of light stop $\tilde{t}_1 - \tilde{\chi}_1^0$ coannihilation as well as light sbottom $\tilde{b}_1 - \tilde{\chi}_1^0$ coannihilation.

We consider these effects for a range of models based on grand unification of the gauge coupling constants: (1) Minimal supergravity model (mSUGRA) [9] where there is universal soft breaking masses at M_G , (2) Nonuniversal supergravity models [10], where the first two generation soft breaking masses are kept universal at M_G (to suppress flavor changing neutral currents) as well as the gaugino masses, but the Higgs and third generation soft breaking masses are allowed to be nonuniversal, and (3) a D-brane model [11] based on Type IIB

strings [12] where soft breaking masses at M_G of the $SU(2)_L$ doublet squark, slepton and Higgs are kept degenerate but distinct from the $SU(2)_L$ singlets, and similarly the gaugino $SU(2)_L$ doublet soft breaking mass is distinct from the $SU(2)_L$ singlets. While the first two models have been characterized as SUGRA models, they can also be realized in string models, and in fact any string model based on grand unification at a high M_G scale with the Standard Model gauge group holding below M_G , phenomenologically can be treated as a SUGRA model with an appropriate amount of nonuniversal soft breaking. Thus the three models sample the possibilities of universal soft breaking, nonuniversal soft breaking in the squark, slepton and Higgs sector but universal gaugino masses, and finally nonuniversality in the gaugino sector as well.

Since the Milky Way is perhaps 90% dark matter, it is a “laboratory” for studying the properties of dark matter (DM). Possible signals for DM include annihilation in the halo of the Galaxy, annihilation in the center of the Sun or Earth, and direct detection from scattering by terrestrial nuclear targets. Of these, the last is most promising, and we restrict our discussion here to this. (For recent discussions of the other possibilities see [13–15]). In general, the neutralino-nucleus scattering has a spin independent and spin dependent part. However, for heavy nuclei (aside from exceptional situations discussed below), the spin independent scattering dominates, giving rise to approximately equal scattering by neutrons (n) and protons (p) in the nucleus. It is thus possible to extract from any data the neutralino-proton cross section, $\sigma_{\tilde{\chi}_1^0-p}$ (subject to astronomical uncertainties about the Milky Way). Current detectors (DAMA, CDMS, UKDMC) are sensitive to cross sections

$$\sigma_{\tilde{\chi}_1^0-p} \gtrsim 1 \times 10^{-6} \text{ pb} \quad (1)$$

with a one to two order of magnitude improvement possible in the near future. Future detectors (e.g. GENIUS, Cryoarray) plan to be sensitive down to

$$\sigma_{\tilde{\chi}_1^0-p} \gtrsim (10^{-9} - 10^{-10}) \text{ pb} \quad (2)$$

and thus it is of interest to see what parts of the SUSY parameter space can be examined by such detectors.

In order to obtain accurate calculations of both the relic density and $\sigma_{\tilde{\chi}_1^0-p}$ for large $\tan\beta$, it is necessary to include a number of corrections in the analysis, and we list these here: (i) In relating the theory at M_G to phenomena at the electroweak scale, the two loop gauge and one loop Yukawa renormalization group equations (RGE) are used, iterating to get a consistent SUSY spectrum. (ii) QCD RGE corrections are further included below the SUSY breaking scale for contributions involving light quarks. (iii) A careful analysis of the light Higgs mass m_h is necessary (including two loop and pole mass corrections) as the current LEP limits impact sensitively on the relic density analysis. (iv) L-R mixing terms are included in the sfermion (mass)² matrices since they produce important effects for large $\tan\beta$ in the third generation. (v) One loop corrections are included to m_b and m_τ which are again important for large $\tan\beta$. (vi) The experimental bounds on the $b \rightarrow s\gamma$ decay put significant constraints on the SUSY parameter space and theoretical calculations here include the leading order (LO) and NLO corrections for large $\tan\beta$. Note that we have not in the following imposed $b-\tau$ (or $t-b-\tau$) Yukawa unification or proton decay constraints as these depend sensitively on unknown post-GUT physics. For example, such constraints do

not naturally occur in the string models where $SU(5)$ (or $SO(10)$) gauge symmetry is broken by Wilson lines at M_G (even though grand unification of the gauge coupling constants at M_G for such string models is still required).

In carrying out the above calculations we have included the latest LEP bound on the light Higgs mass, $m_h > 114$ GeV [16] and the recent NLO corrections for large $\tan\beta$ for the $b \rightarrow s\gamma$ decay [17,18]. (We have checked numerically that [17] and [18] give identical results.) Since there are still some remaining errors in the theoretical calculation of m_h as well as uncertainty in the top quark mass, $m_t = (175 \pm 5)$ GeV, we will conservatively assume here that $m_h > 110$ GeV. In the MSSM, the constraint on m_h is $\tan\beta$ dependent as Ah production (A is the CP odd Higgs) when $m_A \cong M_Z$ is possible for $\tan\beta \gtrsim 9$ and this can be confused with Zh production. However, in SUGRA models, radiative electroweak breaking eliminates this part of the parameter space, and so it is correct to impose the LEP bound on m_h for the full range of $\tan\beta$. LEP also gives the bound [19] $m_{\tilde{\chi}_1^\pm} > 102$ GeV, and the Tevatron bound for the gluino (\tilde{g}) is [20] $m_{\tilde{g}} > 270$ GeV (for squark (\tilde{q}) and gluino masses approximately equal). We assume an allowed 2σ range from the CLEO data for the $b \rightarrow s\gamma$ branching ratio [21]:

$$1.8 \times 10^{-4} \leq B(B \rightarrow X_s \gamma) \leq 4.5 \times 10^{-4} \quad (3)$$

In calculating the relic density we will assume the bounds

$$0.02 < \Omega_{\tilde{\chi}_1^0} h^2 < 0.25 \quad (4)$$

where $\Omega_{\tilde{\chi}_1^0} = \rho_{\tilde{\chi}_1^0}/\rho_c$, $\rho_{\tilde{\chi}_1^0}$ is the relic density of the $\tilde{\chi}_1^0$, $\rho_c = 3H_0^2/8\pi G_N$ (H_0 is the present Hubble constant and G_N is the Newton constant) and $H_0 = h100\text{km s}^{-1}\text{Mpc}^{-1}$. The lower bound on $\Omega_{\tilde{\chi}_1^0} h^2$ is somewhat lower than more conventional estimates ($\Omega_{\tilde{\chi}_1^0} h^2 > 0.1$), and allows us to consider the possibility that not all the DM are neutralinos. (In the following, we will mention when results are sensitive to this lower bound.) Accurate determinations by the MAP and Planck satellites of the dark matter relic density will clearly strengthen the theoretical predictions, and already, analyses using combined data from the CMB, large scale structure, and supernovae data suggests that the correct value of the relic density lies in a relatively narrow band in the center of the region of Eq. (4) [22]. We will here, however, use the conservative range given in Eq. (4).

Supersymmetry theory allows one to calculate the $\tilde{\chi}_1^0$ -quark cross section and we follow the analysis of [23] to convert this to $\tilde{\chi}_1^0 - p$ scattering. For this one needs the πN σ term,

$$\sigma_{\pi N} = \frac{1}{2}(m_u + m_d)\langle p|\bar{u}u + \bar{d}d|p\rangle, \quad (5)$$

$\sigma_0 = \sigma_{\pi N} - (m_u + m_d)\langle p|\bar{s}s|p\rangle$ and the quark mass ratio $r = 2m_s/(m_u + m_d)$. We use here $\sigma_0 = 30$ MeV [24], and $r = 24.4 \pm 1.5$ [25]. Recent analyses, based on new $\pi - N$ scattering data gives $\sigma_{\pi N} \cong 65$ MeV [26]. Older $\pi - N$ data gave $\sigma_{\pi N} \cong 45$ MeV [27]. We will use in most of the analysis below the larger number. If the smaller number is used, it would have the overall effect in most of the parameter space of reducing $\sigma_{\tilde{\chi}_1^0 - p}$ by about a factor of 3. However, in the special situation for $\mu < 0$ where there is a cancellation of matrix elements, the choice of $\sigma_{\pi N}$ produces a more subtle effect, and we will exhibit there results from both values. Some of the results described below have been mentioned earlier in conference talks [28].

There have been in the recent past a number of calculations of $\sigma_{\tilde{\chi}_1^0-p}$ in the literature [24,29–34]. However, none include simultaneously all the corrections discussed above, the large $\tan\beta$ range and the recent LEP m_h bounds. We find general numerical agreement with other calculations for regions of parameter space where the omitted corrections are small.

II. MSUGRA MODEL

We consider in this section the mSUGRA model. This model is the most predictive of the SUGRA models as it depends on only four additional parameters and one sign. These may be chosen as follows: m_0 , the universal scalar soft breaking mass at M_G ; $m_{1/2}$, the universal gaugino mass at M_G (or alternately one may use $m_{\tilde{\chi}_1^0}$ or $m_{\tilde{g}}$ as these quantities approximately scale with $m_{1/2}$, i.e. $m_{\tilde{\chi}_1^0} \simeq 0.4m_{1/2}$ and $m_{\tilde{g}} \simeq 2.8m_{1/2}$); A_0 , the universal cubic soft breaking coupling at M_G ; $\tan\beta = \langle H_2 \rangle / \langle H_1 \rangle$; and $\mu/|\mu|$, the sign of the Higgs mixing parameter μ in the superpotential term $W = \mu H_1 H_2$. We restrict the parameter space as follows:

$$m_0, m_{1/2} < 1 \text{ TeV} \quad (6)$$

$$|A_0/m_{1/2}| < 4 \quad (7)$$

$$2 < \tan\beta < 50 \quad (8)$$

The relic density is calculated by solving the Boltzman equation in the early universe. If the excited SUSY states lie significantly above the $\tilde{\chi}_1^0$, then this takes the standard form [1]:

$$\frac{dn}{dt} = -3Hn - \langle \sigma_{ann} v \rangle (n^2 - n_{eq}^2) \quad (9)$$

where n is the neutralino number density, n_{eq} is its equilibrium value, $\langle \dots \rangle$ means thermal average, σ_{ann} is the annihilation cross section $\tilde{\chi}_1^0 + \tilde{\chi}_1^0 \rightarrow f$ ($f =$ final state), and v is the relative velocity. In this case, the effects of the heavier particles are suppressed by the Boltzman factor. If however, one or more particles, X_i , have masses m_i near the neutralino ($\tilde{\chi}_1^0 \equiv X_1$, $m_{\tilde{\chi}_1^0} \equiv m_1$), coannihilation effects can occur. In this case Eq. (9) holds for the neutralino number density with, however, n_{eq} and σ_{ann} given by [2]

$$n_{eq} = \sum_i n_{ieq} \quad (10)$$

$$\sigma_{ann} = \sum_{i,j} r_i r_j \sigma_{ij}; \quad r_i \equiv \frac{n_{ieq}}{n_{eq}} \quad (11)$$

In the nonrelativistic limit where freezeout occurs, the equilibrium number densities take the form [3,35]

$$n_{ieq} \simeq g_i \left(\frac{m_i T}{2\pi} \right)^{3/2} \exp(-m_i/T) \left[1 + \frac{15T}{8m_i} \right] \quad (12)$$

Here σ_{ij} is the cross section for $X_i + X_j \rightarrow f$ (σ_{11} is the neutralino annihilation cross section) and g_i are the degeneracy factors. In our analysis, we have included all final states that are energetically allowed.

One sees from Eqs. (11,12) that the effects of coannihilation depend simultaneously on the near degeneracy of any heavier particle with the neutralino, and on the size of the annihilation cross sections. A large cross section can then compensate partially for the Boltzman factor. In SUGRA models two effects occur which enhance the coannihilation for the sleptons. First, since the neutralino is a Majorana particle, its annihilation cross section is p-wave suppressed. Consequently,

$$\sigma_{ij}, \sigma_{i1} \simeq O[10\sigma_{11}]; \quad i, j = \text{sleptons} \quad (13)$$

and the slepton cross sections are enhanced relative to the neutralino cross sections σ_{11} . Second, a numerical accident allows the selectrons to be nearly degenerate with the neutralino over a region of parameter space of increasing $m_0, m_{1/2}$. One can see this analytically for low and intermediate $\tan\beta$ for mSUGRA where the RGE can be solved analytically [36]. At the electroweak scale one has

$$\tilde{m}_{e_R}^2 = m_0^2 + (6/5)f_1 m_{1/2}^2 - \sin^2\theta_W M_W^2 \cos(2\beta) \quad (14)$$

$$m_{\tilde{\chi}_1^0} = (\alpha_1/\alpha_G)m_{1/2} \quad (15)$$

where $f_i = [1 - (1 + \beta_i t)^{-2}]/\beta_i$, $t = \ln(M_G/M_Z)^2$ and β_1 is the $U(1)$ β function. Numerically this gives for e.g. $\tan\beta = 5$

$$\begin{aligned} \tilde{m}_{e_R}^2 &= m_0^2 + 0.15m_{1/2}^2 + (37 \text{ GeV})^2 \\ m_{\tilde{\chi}_1^0}^2 &= 0.16m_{1/2}^2 \end{aligned} \quad (16)$$

Thus for $m_0 = 0$, the \tilde{e}_R becomes degenerate with the $\tilde{\chi}_1^0$ at $m_{1/2} = 370$ GeV, i.e. coannihilation effects begin at $m_{1/2} \simeq (350 - 400)$ GeV. For larger $m_{1/2}$, the near degeneracy is maintained by increasing m_0 , and there is a corridor in the $m_0 - m_{1/2}$ plane allowing for an adequate relic density. (This is in accord with the numerical calculations of [30].)

For larger $\tan\beta$, the situation is more complicated, as the the L-R mixing in the $\tilde{\tau}_1$ (mass²) matrix, generally makes the $\tilde{\tau}_1$ the lightest slepton (lighter than the \tilde{e}_R or $\tilde{\mu}_R$), and hence the $\tilde{\tau}_1$ dominates the coannihilation phenomena. The RGE must of course now be solved numerically, and there is strong sensitivity to A_0 .

FIGURES

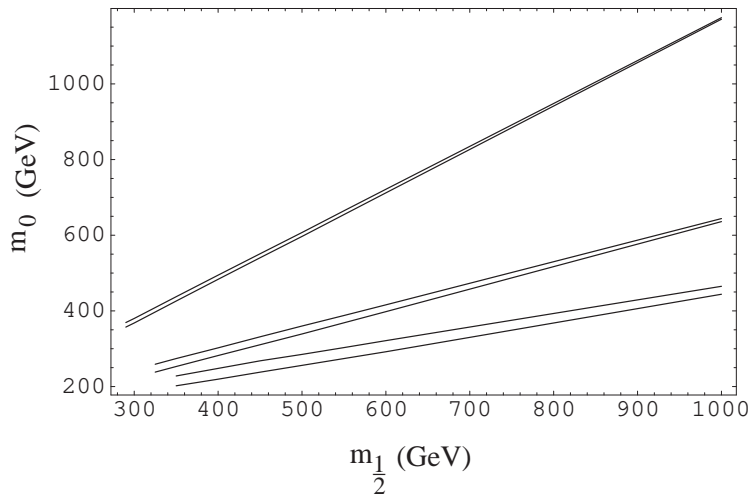


FIG. 1. Allowed corridors in mSUGRA in the $m_0 - m_{1/2}$ plane satisfying the relic density constraint for $\mu > 0$, $\tan \beta = 40$ for (from bottom to top) $A_0 = m_{1/2}$, $2 m_{1/2}$, $4m_{1/2}$. The corridors terminate at low $m_{1/2}$ due to the $b \rightarrow s\gamma$ constraint.

The new effects are exhibited in Fig. 1 where the allowed regions in the $m_0 - m_{1/2}$ plane satisfying Eq. (4) for $A_0 = m_{1/2}$, $2m_{1/2}$ and $4m_{1/2}$ are shown for $\mu > 0$ and $\tan \beta = 40$. One sees several features of the large $\tan \beta$ region there. First, the allowed corridors are sensitive to the value of A_0 , the allowed values of m_0 increasing with A_0 . Further, the corridors end at a minimum value of $m_{1/2}$ due to the $b \rightarrow s\gamma$ constraint. (We note that these lower bounds on $m_{1/2}$ are sensitive to the NLO corrections to the $b \rightarrow s\gamma$ branching ratio mentioned in Sec. 1 above.) In fact, there is only the coannihilation region left in the parameter space, since the $b \rightarrow s\gamma$ constraint at large $\tan \beta$ has eliminated the non coannihilation part of the parameter space. (Actually, there can be small islands of allowed parameter space left in the non coannihilation region ($m_{1/2} \lesssim 350$ GeV) for large $\tan \beta$ due to a cancellation that can occur between the Standard Model amplitude and the chargino amplitude.) While for low $\tan \beta$, m_0 is generally small [30] ($m_0 \lesssim 200$ GeV), we see that at large $\tan \beta$, m_0 can become quite large reaching up to 1 TeV for large A_0 . Finally we mention that while for fixed A_0 the allowed corridors are relatively narrow, as one allows A_0 to vary from small to large values, the allowed region due to coannihilation covers most of the $m_0 - m_{1/2}$ plane.

We turn next to consider the $\tilde{\chi}_1^0 - p$ cross section. Large cross sections can arise for large $\tan \beta$ and small $m_{\tilde{\chi}_1^0}$, and in [33], it was shown that Eq. (1) could be satisfied in mSUGRA only also for small $\Omega_{\tilde{\chi}_1^0} h^2$, i. e. for

$$\tan \beta \gtrsim 25, \quad \Omega_{\tilde{\chi}_1^0} h^2 \lesssim 0.1, \quad m_{\tilde{\chi}_1^0} \lesssim 90 \text{ GeV} \quad (17)$$

Small cross sections generally arise for small $\tan \beta$, large m_0 and large $m_{1/2}$. It is of interest to see what the minimum cross section predicted by theory is in order to know how much of the SUSY parameter space will be examined by proposed detectors. In order to see the effects of coannihilation, we first examine the domain $m_{1/2} < 350$ GeV ($m_{\tilde{\chi}_1^0} < 140$ GeV) where coannihilation does not take place. Fig. 2 exhibits the minimum cross section for $\tan \beta = 6$, $\mu > 0$, satisfying all the accelerator and relic density constraints. One sees that

$\sigma_{\tilde{\chi}_1^0-p} \gtrsim 1 \times 10^{-9}$ pb for $\tan \beta > 6$, and so the entire parameter space in this region would be accessible to detectors planned with sensitivity of Eq. (2).

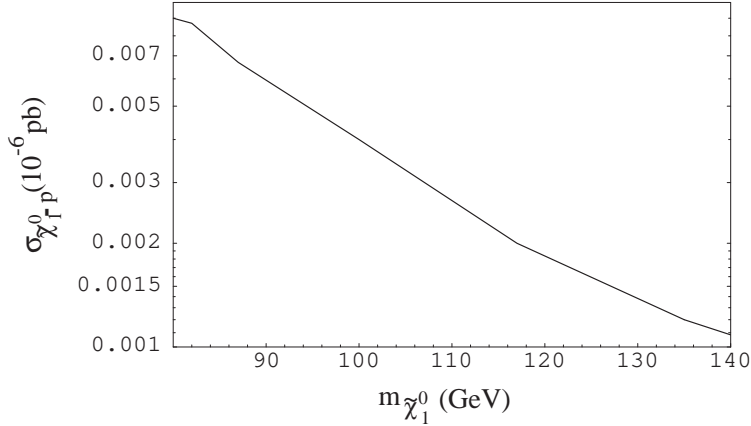


FIG. 2. $(\sigma_{\tilde{\chi}_1^0-p})_{\min}$ in the noncoannihilation region as a function of $m_{\tilde{\chi}_1^0}$ for mSUGRA for $\mu > 0$, $\tan \beta = 6$, obtained by varying over the range of m_0 and A_0 .

At higher $m_{1/2}$, coannihilation occurs, allowing m_0 and $m_{1/2}$ to become larger, and hence the cross section should become smaller. We examine first the case $\mu > 0$. The A_0 dependence at large $\tan \beta$ shown in Fig. 1 then implies that the cross section should also decrease with increasing A_0 , since, as seen in Fig. 1, m_0 then increases. This is seen explicitly in Fig. 3.

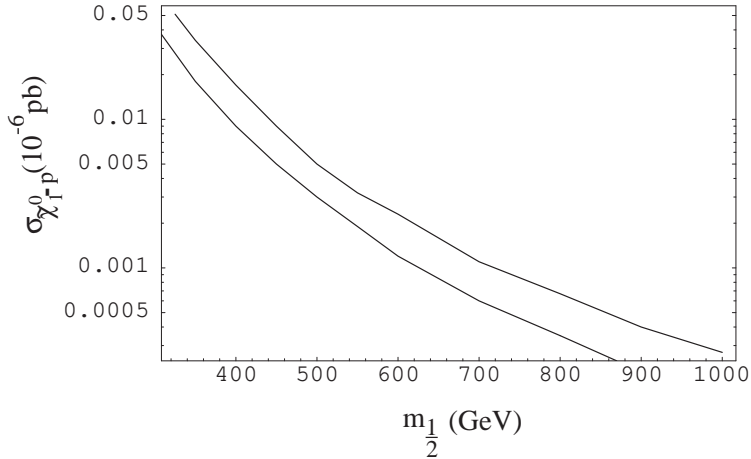


FIG. 3. $\sigma_{\tilde{\chi}_1^0-p}$ as a function of $m_{1/2}$ for mSUGRA $\mu > 0$, $\tan \beta = 40$ and $A_0 = 2m_{1/2}$ (upper curve), $4m_{1/2}$ (lower curve).

Thus it is possible that as $m_{1/2}$ gets large, a consequence of coannihilation is that large $\tan \beta$ and large A_0 can give smaller cross sections than low $\tan \beta$. This is illustrated in Fig. 4 where $\sigma_{\tilde{\chi}_1^0-p}$ is plotted as a function of $m_{1/2}$ for $A_0 = 4m_{1/2}$, $\tan \beta = 40$ (upper curve) and $\tan \beta = 3$ (lower curve). One sees that for $m_{1/2} > 600$ GeV, the $\tan \beta = 40$ curve actually drops below the $\tan \beta = 3$ curve, the A_0 dependence (producing large m_0) compensating for the $\tan \beta$ dependence. One has however, the bound

$$\sigma_{\tilde{\chi}_1^0-p} \gtrsim 1 \times 10^{-10} \text{ pb, for } \mu > 0, m_{1/2} < 1 \text{ TeV} \quad (18)$$

Again, most of this parameter space will be within the reach of planned future detectors.

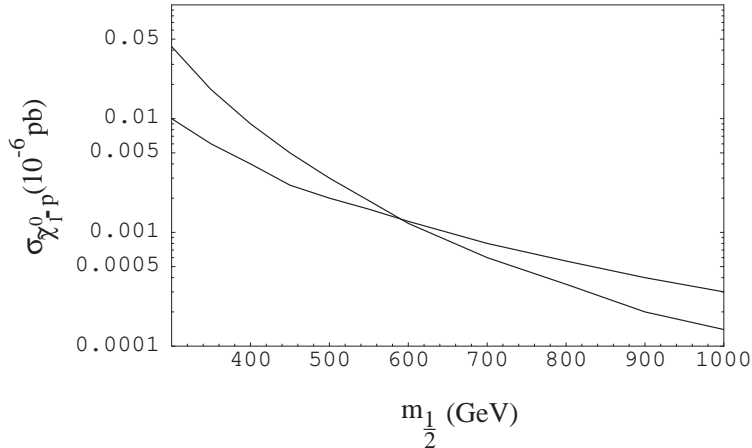


FIG. 4. $\sigma_{\tilde{\chi}_1^0-p}$ as a function of $m_{1/2}$ for mSUGRA, $\mu > 0$ for $A_0 = 4 m_{1/2}$, $\tan \beta = 40$ (upper left curve), $\tan \beta = 3$ (lower left curve).

We turn next to the case of $\mu < 0$. The situation here is more complicated. As pointed out for low and intermediate $\tan \beta$ in [31], an accidental cancellation can occur between the Higgs u -quark and the Higgs d -quark scattering amplitudes which can greatly reduce $\sigma_{\tilde{\chi}_1^0-p}$ and we investigate here whether this cancellation continues to occur in the high $\tan \beta$ region. Since the cancellation is somewhat subtle, we briefly describe how it comes about. In general, $\tilde{\chi}_1^0$ is a mixture of Bino(\tilde{B}), Wino(\tilde{W}) and the two Higgsinos (\tilde{H}_1, \tilde{H}_2):

$$\tilde{\chi}_1^0 = N_{11}\tilde{B} + N_{12}\tilde{W} + N_{13}\tilde{H}_1 + N_{14}\tilde{H}_2 \quad (19)$$

where N_{1i} are the amplitudes. In much of the parameter space, the t -channel Higgs exchanges (h, H) dominate $\sigma_{\tilde{\chi}_1^0-p}$. The d and u quark Higgs amplitudes are [37]

$$A^d = \frac{g_2^2 m_d}{2M_W} \left(-\frac{\sin \alpha}{\cos \beta} \frac{F_h}{m_h^2} + \frac{\cos \alpha}{\cos \beta} \frac{F_H}{m_H^2} \right) \quad (20)$$

$$A^u = \frac{g_2^2 m_u}{2M_W} \left(\frac{\cos \alpha}{\sin \beta} \frac{F_h}{m_h^2} + \frac{\sin \alpha}{\sin \beta} \frac{F_H}{m_H^2} \right) \quad (21)$$

where α is the Higgs mixing angle and

$$F_h = (N_{12} - N_{11} \tan \theta_W)(N_{14} \cos \alpha + N_{13} \sin \alpha) \quad (22)$$

$$F_H = (N_{12} - N_{11} \tan \theta_W)(N_{14} \sin \alpha - N_{13} \cos \alpha) \quad (23)$$

Since the s -quark contribution to the scattering is quite large, the d -quark amplitude A^d will generally be quite large. However A^d will be suppressed if the amplitudes N_{13}, N_{14} obey the equation

$$N_{14} \simeq -N_{13} \frac{\tan \alpha + \frac{m_h^2}{m_H^2} \cot \alpha}{1 + \frac{m_h^2}{m_H^2}} \quad (24)$$

In general $\tan \alpha$ is negative and small ($\tan \alpha \simeq -\cot \beta \simeq -0.1$), and Eq. (24) can happen if N_{14}/N_{13} is positive, which is the case for $\mu < 0$. Once A^d is sufficiently suppressed, it can

cancel the remaining (smaller) u -quark contribution coming from A^u , leading to a nearly zero value of $\sigma_{\tilde{\chi}_1^0-p}$. For fixed $\tan\beta$, total cancellation occurs at a fixed value of $m_{1/2}$, though the effects of cancellation has a width. What happens is shown in Fig. 5 where $\sigma_{\tilde{\chi}_1^0-p}$ is plotted in the large $m_{1/2}$ region for $\tan\beta = 6$ (short dash), $\tan\beta = 8$ (dotted), $\tan\beta = 10$ (solid), $\tan\beta = 20$ (dot-dash) and $\tan\beta = 25$ (dashed). One sees that the cross section dips sharply when $\tan\beta$ is increased from 6 to 8, and goes through a minimum for $\tan\beta = 8$ at $m_{1/2} \simeq 810$ GeV. For $\tan\beta = 10$, the minimum recedes to $m_{1/2} \simeq 725$ GeV, and then begins to advance for higher $\tan\beta$ i.e. rising to $m_{1/2} \simeq 830$ GeV for $\tan\beta = 20$, and $m_{1/2} \simeq 950$ GeV for $\tan\beta = 25$. Thus if we restrict $m_{1/2}$ to be below 1 TeV, the cross section will fall below the sensitivity of the planned future detectors for $m_{1/2} \gtrsim 450$ GeV for a restricted region of $\tan\beta$ i. e.

$$\sigma_{\tilde{\chi}_1^0-p} < 1 \times 10^{-10} \text{ pb for } 450 \text{ GeV} < m_{1/2} < 1 \text{ TeV}; 5 \lesssim \tan\beta \lesssim 30 \quad (25)$$

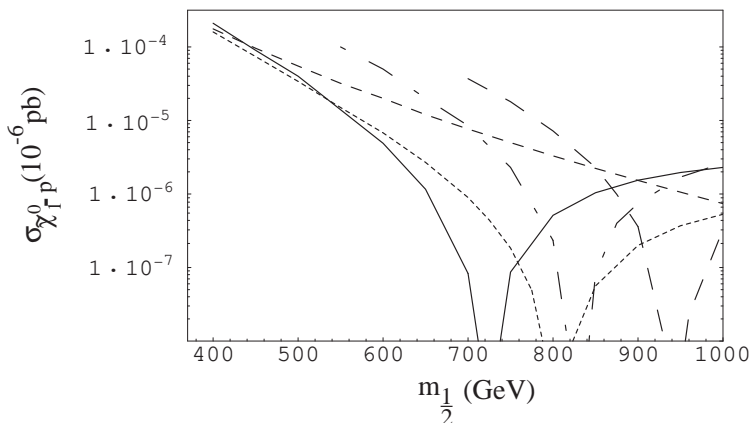


FIG. 5. $\sigma_{\tilde{\chi}_1^0-p}$ for mSUGRA for $\mu < 0$, $A_0 = 1500$ GeV, for $\tan\beta = 6$ (short dash), $\tan\beta = 8$ (dotted), $\tan\beta = 10$ (solid), $\tan\beta = 20$ (dot-dash), $\tan\beta = 25$ (dashed). Note that the $\tan\beta = 6$ curve terminates at low $m_{1/2}$ due to the Higgs mass constraint, and the other curves terminate at low $m_{1/2}$ due to the $b \rightarrow s\gamma$ constraint.

At the minimum, the cross sections can become quite small, e. g. $< 1 \times 10^{-13}$ pb, without major fine tuning of parameters, corresponding to an almost total cancellation. (Actually, as pointed out in [38], the true minimum of the cross section would then arise from the spin dependent part of the scattering, which though very small, does not possess the same cancellation phenomena.) Further, the widths of the minima for fixed $\tan\beta$ are fairly broad. While in this domain the proposed detectors obeying Eq. (2) will not be able to observe Milky Way wimps, mSUGRA would imply that the squarks and gluino would lie above 1 TeV, but at masses that would still be accessible to the LHC (i.e. < 2.5 TeV). Also note that this phenomena occurs only for $\mu < 0$ and for a restricted range of $\tan\beta$, so cross checks of the theory would still be available.

The minima occurring in Fig. 5 arose from cancellations between the Higgs u -quark and Higgs d -quark amplitudes, and as such are sensitive to the quark content of the proton. As discussed in Sec. 1, $\sigma_{\pi N}$ is not yet well determined, and Fig. 5 used $\sigma_{\pi N} = 65$ MeV. In Fig. 6, we compare this choice (solid curve) for $\tan\beta = 10$ with the parameters used in [27,31] (dashed curve), where $\sigma_{\pi N} = 45$ MeV. One sees that the minimum at $m_{1/2} = 725$

GeV is shifted to $m_{1/2} = 600$ GeV, with analogous shifts occurring for the other values of $\tan\beta$. Thus the extreme cancellations that occur in the coannihilation region for $\mu < 0$ are quite sensitive to the properties of the proton.

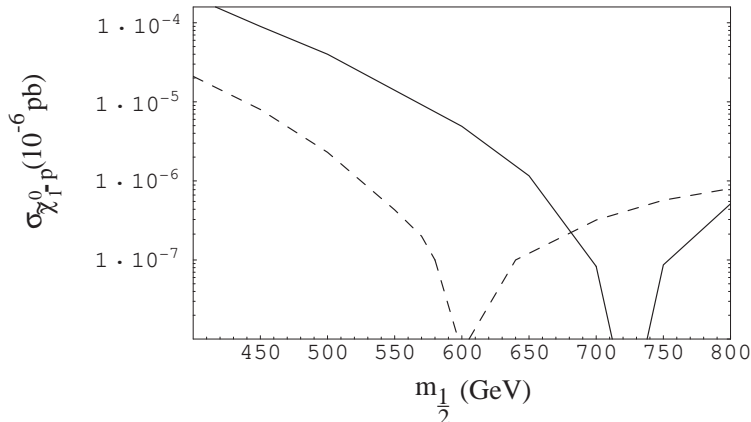


FIG. 6. $\sigma_{\tilde{\chi}_1^0-p}$ for mSUGRA for $\mu < 0$, $\tan\beta = 10$, $A_0 = 1500$ GeV for $\sigma_{\pi N} = 65$ MeV (solid curve) and the parameters of [26,36] (dashed curve) where $\sigma_{\pi N} = 45$ MeV was used.

III. SUGRA MODELS WITH NONUNIVERSAL SOFT BREAKING

We consider here models with nonuniversal soft breaking masses. In order to suppress flavor changing neutral currents, we maintain the universal soft breaking slepton and squark masses, m_0 , at M_G in the first two generations. However, experiment is compatible with nonuniversal Higgs and third generation soft breaking at M_G , and these can arise from nonuniversal couplings in the supergravity Kahler potential. We parameterize this situation as follows:

$$\begin{aligned}
 m_{H_1}^2 &= m_0^2(1 + \delta_1); & m_{H_2}^2 &= m_0^2(1 + \delta_2); \\
 m_{q_L}^2 &= m_0^2(1 + \delta_3); & m_{t_R}^2 &= m_0^2(1 + \delta_4); & m_{\tau_R}^2 &= m_0^2(1 + \delta_5); \\
 m_{b_R}^2 &= m_0^2(1 + \delta_6); & m_{l_L}^2 &= m_0^2(1 + \delta_7).
 \end{aligned}
 \tag{26}$$

where $q_L = (\tilde{t}_L, \tilde{b}_L)$ squarks, $l_L = (\tilde{\nu}_\tau, \tilde{\tau}_L)$ sleptons etc. The δ_i measure the deviations from universality. (If one were to impose $SU(5)$ or $SO(10)$ symmetry then $\delta_3 = \delta_4 = \delta_5 \equiv \delta_{10}$, and $\delta_6 = \delta_7 \equiv \delta_5$.) In the following we limit the δ_i to obey

$$-1 < \delta_i < +1 \tag{27}$$

The lower bound is necessary to prevent tachyons at M_G , and the upper bound represents a naturalness condition. We maintain gauge coupling constant unification at M_G (which is in accord with LEP data). We also assume here gaugino mass unification. (Deviations from this can arise from nonuniversal couplings in the supergravity gauge function f_{ab} , and an example of this is treated in the next section.)

While the nonuniversal models contain a number of additional parameters, one can obtain an understanding of the new effects these imply from the following analytical considerations. In the decomposition of Eq. (19), the lightest neutralino is mostly Bino, i.e. $N_{11} \gtrsim 0.8$. The

Higgs mixing parameter μ to a large extent controls this mix, and as μ^2 decreases (increases) the higgsino content increases (decreases). In order to see qualitatively what happens we examine the low and intermediate $\tan\beta$ region where the RGE can be solved analytically. One finds for μ^2 the result (see e.g. [39]):

$$\begin{aligned} \mu^2 = & \frac{t^2}{t^2-1} \left[\left(\frac{1-3D_0}{2} + \frac{1}{t^2} \right) + \frac{1-D_0}{2} (\delta_3 + \delta_4) \right. \\ & \left. - \frac{1+D_0}{2} \delta_2 + \frac{\delta_1}{t^2} \right] m_0^2 + \text{universal parts} + \text{loop corrections.} \end{aligned} \quad (28)$$

where $t = \tan\beta$, and $D_0 \cong 1 - (m_t/200\text{GeV} \sin\beta)^2 \cong 0.25$. One sees that the universal contribution to the m_0^2 term in μ^2 is small, making μ^2 quite sensitive to nonuniversal contributions. Also since D_0 is small, the Higgs and squark nonuniversalities enter coherently, approximately in the combination $\delta_3 + \delta_4 - \delta_2$. (The RGE can also be solved analytically for the SO(10) model where $\tan\beta > 40$, and numerically otherwise, with results qualitatively similar to Eq. (28).) In addition we note here the mass of the CP odd Higgs boson, m_A is

$$\begin{aligned} m_A^2 = & \frac{t^2+1}{t^2-1} \left[\frac{3(1-D_0)}{2} + \frac{1-D_0}{2} (\delta_3 + \delta_4) \right. \\ & \left. - \frac{1+D_0}{2} \delta_2 + \delta_1 \right] m_0^2 + \text{universal parts} + \text{loop corrections.} \end{aligned} \quad (29)$$

The effects of the nonuniversalities can be seen to fall into the following categories:

(i) The spin independent neutralino-proton cross section depends upon the interference between the gaugino and higgsino parts of the neutralino, the larger the amount of interference the larger the cross section. Thus $\sigma_{\tilde{\chi}_1^0-p}$ can be significantly increased relative to mSUGRA by decreasing μ^2 (and hence increasing the higgsino content) by choosing $\delta_3, \delta_4, \delta_1 < 0, \delta_2 > 0$, and be decreased (though by not so large amount) with the opposite sign choice.

(ii) In the early universe annihilation cross section, the s-channel Z^0 pole amplitude depends on the higgsino contribution of the neutralino (the Bino and Wino parts giving zero coupling). Thus if μ^2 is lowered by choosing $\delta_3, \delta_4, \delta_1 < 0, \delta_2 > 0$ one gets an increased amount of annihilation, and a decreased amount with the opposite choice of signs. Thus deviations from universality can significantly effect the satisfaction of the relic density constraints of Eq. (4).

(iii) The third generation squark and slepton nonuniversalities shift the mass spectrum of the particles. Thus the positions of the corridors of coannihilation, and their widths can be significantly modified (also modifying the cross section $\sigma_{\tilde{\chi}_1^0-p}$.)

Effects of type (i) were early observed in [39], and further discussed in [33] where it was seen that $\sigma_{\tilde{\chi}_1^0-p}$ could be increased by a factor of 10 or more with the sign choice $\delta_{3,4,1} < 0, \delta_2 > 0$. We here update this result to take into account of the latest LEP bound $m_h > 114$ GeV. Fig. 7 shows the maximum value of $\sigma_{\tilde{\chi}_1^0-p}$ for the nonuniversal models for $\mu > 0$ with the above choice of signs for δ_i for $\tan\beta = 7$ (lower curve) and $\tan\beta = 12$ (upper curve). One sees that detectors obeying Eq. (1) are sampling the parameter space with $\tan\beta \geq 7$ (compared with the mSUGRA result of $\tan\beta \geq 25$).

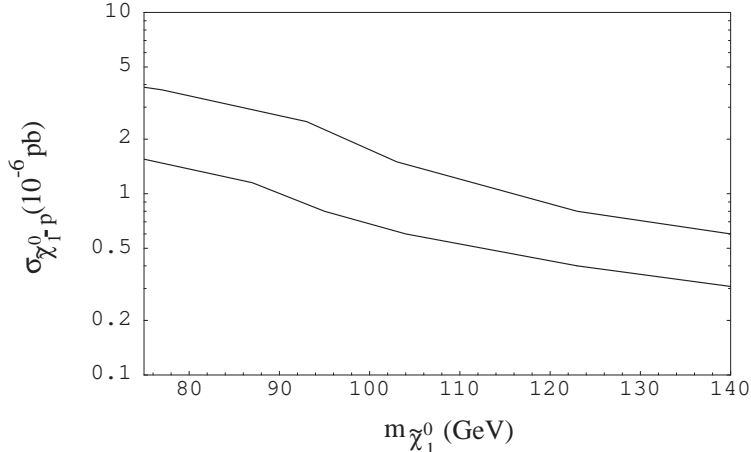


FIG. 7. Maximum value of $\sigma_{\tilde{\chi}_1^0-p}$ as a function of $m_{\tilde{\chi}_1^0}$ for the nonuniversal model with $\mu > 0$, $\delta_1, \delta_3, \delta_4 < 0$, $\delta_2 > 0$. The lower curve is for $\tan\beta = 7$, the upper curve is for $\tan\beta = 12$.

To illustrate further some of the effects of nonuniversality, we consider first the case where there are only Higgs mass nonuniversal soft breaking, i.e. only $\delta_{1,2}$ are non zero. In general for the universal mSUGRA case, both μ^2 and m_A are determined in terms of the other SUSY parameters. From Eqs. (28) and (29), we see that these quantities now depend on the additional parameters δ_1 and δ_2 , and thus may be varied keeping the other (mSUGRA) parameters m_0 , $m_{1/2}$, A_0 and $\tan\beta$ fixed. In [40], it was thus assumed that μ^2 and m_A could be chosen arbitrarily. Actually, however, both μ^2 and m_A are constrained by the bounds of Eq. (27), and varying μ^2 and m_A arbitrarily can lead to points in parameter space with unreasonably large values of $\delta_{1,2}$ (or even tachyonic values with $\delta_{1,2} < -1$). Thus here we will examine the actual parameter space subject to the conditions of Eq. (27) (as well as the usual relic density and accelerator bounds). As an example of an effect of type (ii), we consider in Fig.8 the case in the coannihilation region where $A_0 = m_{1/2}$, $\tan\beta = 40$, and chose $\delta_2 = 1$. Since μ^2 is insensitive to δ_1 we set $\delta_1 = 0$. In this domain, the allowed stau coannihilation region corresponds to the lowest band in the $m_0 - m_{1/2}$ plane of Fig. 1, with m_0 running from about 200 GeV to 400 GeV and the corresponding corridor is only slightly effected by $\delta_2 \neq 0$. As shown in Fig. 8, the effect of the nonuniversal soft breaking now allows the opening up of a new wide band of allowed region at much higher values of m_0 . Thus normally such large values of m_0 would give rise to too little annihilation to satisfy Eq. (4). However, by lowering μ^2 and hence raising the higgsino content of the neutralino, the Z^0 channel annihilation is enhanced allowing for an acceptable relic density. In Fig. 8, the low side of the band corresponds to $\Omega_{\tilde{\chi}_1^0} h^2 = 0.25$, while the upper end to $\Omega_{\tilde{\chi}_1^0} h^2 = 0.02$. If one were to raise the relic density lower bound to $\Omega_{\tilde{\chi}_1^0} h^2 = 0.1$, the width of the band would be reduced by about 30% to 40%. (The small dip at $m_{1/2} = (400 - 450)$ GeV (i.e. $m_{\tilde{\chi}_1^0} = (160 - 180)$ GeV) arises due to the opening of the $t - \bar{t}$ channel in the annihilation cross section.) Thus we see that nonuniversal soft breaking allows for much larger values of m_0 than mSUGRA and hence a heavier mass spectrum, and this could be an experimental signal for nonuniversalities. (Universal soft breaking only allows for the coannihilation corridor in Fig. 8 at much lower m_0 .) In addition, the larger m_0 leads to a smaller $\sigma_{\tilde{\chi}_1^0-p}$.

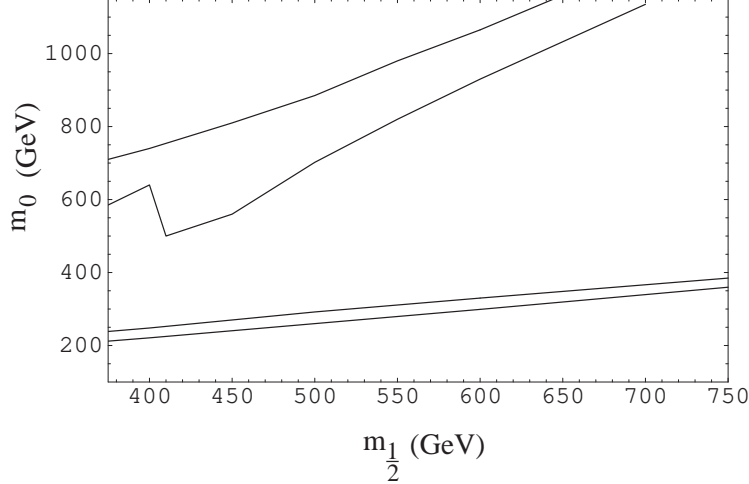


FIG. 8. Effect of a nonuniversal Higgs soft breaking mass enhancing the Z^0 s-channel pole contribution in the early universe annihilation, for the case of $\delta_2 = 1$, $\tan \beta = 40$, $A_0 = m_{1/2}$, $\mu > 0$. The lower band is the usual $\tilde{\tau}_1$ coannihilation region. The upper band is an additional region satisfying the relic density constraint arising from increased annihilation via the Z^0 pole due to the decrease in μ^2 increasing the higgsino content of the neutralino.

We consider a second example where both effects of type (ii) and (iii) occur simultaneously, by examining third generation squark and slepton nonuniversal masses obtained when δ_{10} ($= \delta_3 = \delta_4 = \delta_5$) takes on the value $\delta_{10} = -0.7$. (All other δ_i are chosen zero.) We again assume $A_0 = m_{1/2}$, $\tan \beta = 40$ and $\mu > 0$. The effect of δ_{10} is shown in Fig. 9. The lowest band is the usual mSUGRA $\tilde{\tau}_1$ coannihilation band (shown here for reference only). The upper band corresponds to two phenomena: The lower half is the actual $\tilde{\tau}_1$ coannihilation region which has been shifted upwards due to the fact that m_0^2 for the $\tilde{\tau}_1$ has been replaced by $m_0^2(1 + \delta_{10})$, and since δ_{10} is negative, one needs a larger m_0 to achieve the coannihilation corridor. The upper part corresponds to the opening of the Z^0 channel as in Fig. 8 since $\delta_{10} < 0$ reduces μ^2 increasing the higgsino content of the neutralino. For $m_{1/2} \lesssim 500$ GeV, the two bands overlap. However at higher $m_{1/2}$, they are separated. Thus in the high $m_{1/2}$ region, the low side of the middle band (where $\tilde{\tau}_1$ coannihilation is occurring) corresponds to $\Omega_{\tilde{\chi}_1^0} h^2 = 0.02$, while the upper side corresponds to $\Omega_{\tilde{\chi}_1^0} h^2 = 0.25$. In the region between the two top bands, $\Omega_{\tilde{\chi}_1^0} h^2 > 0.25$ (and hence excluded). Finally, since δ_3 and δ_4 are negative (reducing μ^2 and also making the total m_0^2 contribution to μ^2 negative), for sufficiently large m_0 , the Z^0 channel opens reducing $\Omega_{\tilde{\chi}_1^0} h^2$ to 0.25 on the lower side of the top band, that band terminating when $\Omega_{\tilde{\chi}_1^0} h^2 = 0.02$ on the top.

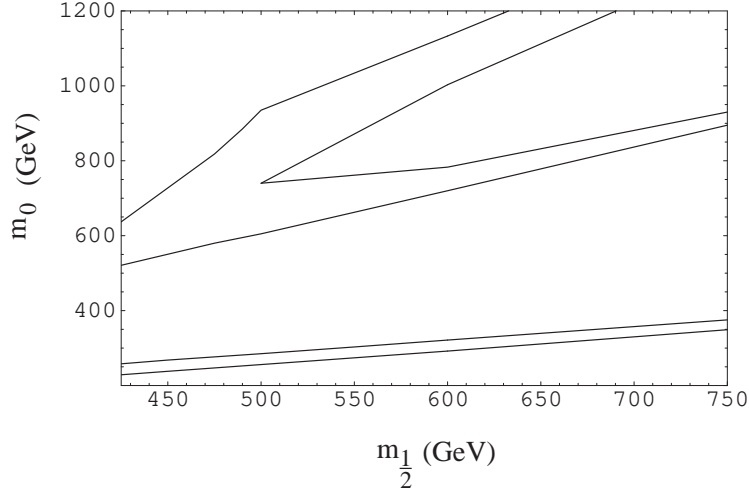


FIG. 9. Allowed regions in the $m_0 - m_{1/2}$ plane for the case $\tan \beta = 40$, $A_0 = m_{1/2}$, $\mu > 0$. The bottom curve is the mSUGRA $\tilde{\tau}_1$ coannihilation band of Fig. 1 (shown for reference). The middle band is the actual $\tilde{\tau}_1$ coannihilation band when $\delta_{10} = -0.7$. The top band is an additional allowed region due to the enhancement of the Z^0 s-channel annihilation arising from the nonuniversality lowering the value of μ^2 and hence raising the higgsino content of the neutralino. For $m_{1/2} \lesssim 500$ GeV, the two bands overlap.

We note in both Figs. 8 and 9, that the effect of nonuniversalities can greatly enhance the allowed region in the $m_0 - m_{1/2}$ plane for large $m_{1/2}$, particularly by increasing m_0 , and these changes occur without unreasonable amounts of nonuniversality.

We consider next the neutralino-proton cross sections arising in these nonuniversal soft breaking cases. One might have expected that the new regions in the $m_0 - m_{1/2}$ plane allowed by the relic density constraint would correspond to smaller values of $\sigma_{\tilde{\chi}_1^0-p}$ since they are bands of much larger m_0 . However this is compensated by the fact that the nonuniversal effects considered above also reduce μ^2 and effects of type (i) compensate for the largeness of m_0 and in fact give a net increase to the cross section. This is illustrated for the example of Fig. 8 in Fig. 10 where $\sigma_{\tilde{\chi}_1^0-p}$ is plotted for $\delta_2 = 1$, $\tan \beta = 40$, $A_0 = m_{1/2}$. The solid line corresponds to the cross section for the $\tilde{\tau}_1$ coannihilation corridor (the lower band of Fig.8), while the long (short) dashed curves correspond to the cross sections along the top (bottom) of the Z^0 pole band. We see that the Z^0 band cross sections, where m_0 is very large, are quite large, and this region of parameters should soon be accessible to e.g. to the next phase of the CDMS experiment in the Soudan mine. The cross section in the lower m_0 domain corresponding to the $\tilde{\tau}_1$ coannihilation region are much smaller, and to explore this domain would require e.g. the GENIUS or Cryoarray detectors.

In Fig. 11, we examine the expected neutralino-proton cross section for the case of $\delta_{10} = -0.7$, $\tan \beta = 40$, $A_0 = m_{1/2}$, $\mu > 0$ of Fig. 9. Here the large dashed curve is the cross section running along the top of the upper band of Fig. 9 (the top of the Z^0 channel band) and the short dashed curve is the cross section along the bottom of the middle band (the bottom of the $\tilde{\tau}_1$ coannihilation corridor). The solid curve is shown for comparison and would be the cross section in the $\tilde{\tau}_1$ coannihilation corridor for universal soft breaking (mSUGRA). We see again that the Z^0 corridor with very large m_0 would be accessible to the CDMS Soudan experiment. The actual $\tilde{\tau}_1$ coannihilation corridor cross section lies

considerably higher than the universal case, but would probably require the GENIUS or Cryoarray detectors to explore.

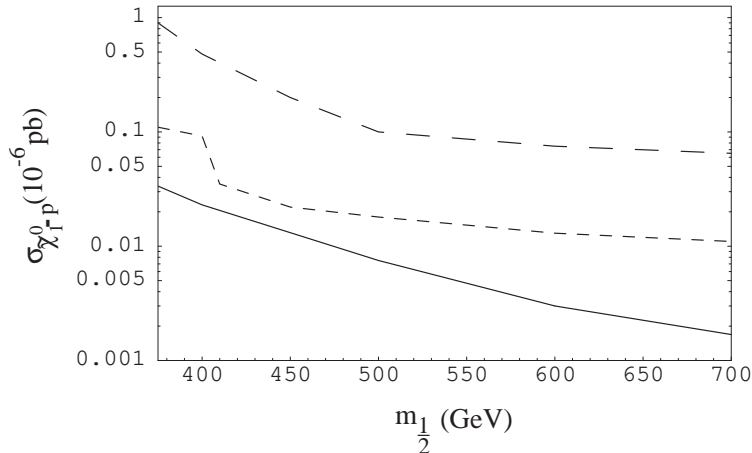


FIG. 10. $\sigma_{\tilde{\chi}_1^0-p}$ as a function of $m_{1/2}$ for $\delta_2 = 1$ (other $\delta_i = 0$), for $\tan\beta = 40$, $A_0 = m_{1/2}$, $\mu > 0$. The long (short) dashed curves are the cross sections along the upper (lower) sides of the Z^0 bands of Fig. 8. The solid curve is $\sigma_{\tilde{\chi}_1^0-p}$ along the $\tilde{\tau}_1$ coannihilation corridor of Fig. 8.

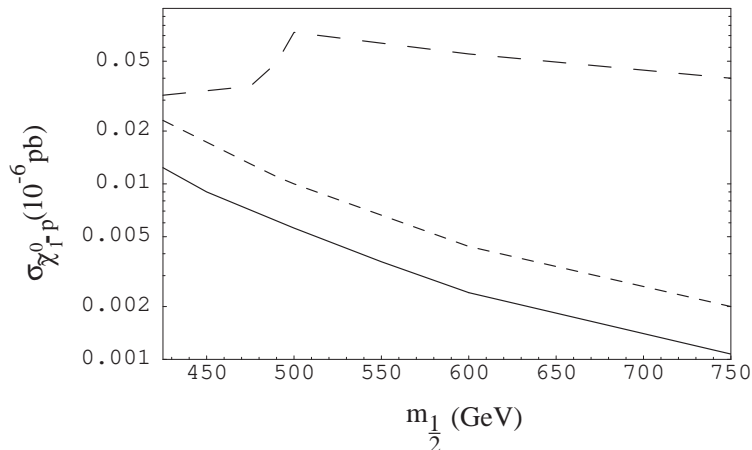


FIG. 11. $\sigma_{\tilde{\chi}_1^0-p}$ as a function of $m_{1/2}$ for $\delta_{10} = -0.7$ (other $\delta_i = 0$), for $\tan\beta = 40$, $A_0 = m_{1/2}$, $\mu > 0$. The long dashed curve is the cross section along the top of the upper band in Fig. 9 where Z^0 annihilation is occurring. (The reduction at $m_{1/2} \lesssim 500$ GeV is due to the $b \rightarrow s\gamma$ constraint.) The short dashed curve is the cross section along the bottom of the middle band where $\tilde{\tau}_1$ coannihilation effects occur for this nonuniversal model. The solid curve is included for comparison and is the cross section in the $\tilde{\tau}_1$ coannihilation corridor for the case of universal soft breaking (mSUGRA).

In the above discussion, we have chosen the signs of the δ_i parameters to decrease μ^2 to illustrate the dramatic effects such δ_i can produce without any unusually large amount of nonuniversality. If instead one were to choose the opposite signs, e.g. $\delta_2 < 0$, or $\delta_{10} > 0$, the μ^2 would have been increased. For this region of parameter space the Z^0 annihilation channel would now be absent (as in mSUGRA). The usual $\tilde{\tau}_1$ coannihilation corridors would of course still be present, but for the $\delta_{10} > 0$ case at lower values of m_0 . The cross sections

for $\mu > 0$ would then be somewhat reduced, but still accessible to future detectors.

The cross sections discussed above were for $\mu > 0$. We now consider the $\mu < 0$ case. In the mSUGRA model, it was seen that for large $m_{1/2}$ with $m_{1/2} < 1$ TeV and a restricted range of $\tan \beta$, a special cancellation could occur which reduced $\sigma_{\tilde{\chi}_1^0-p}$ to be below 10^{-12} pb (see Fig. 5), well below what future detectors could see. This cancellation involved the Higgs u -quark and Higgs d -quark amplitudes, when the neutralino components obey Eq. (24). However, nonuniversal choices such as those of Figs. (8-11), involve now two region of parameter space consistent with the relic density bounds: the coannihilation region, and the region above it dominated by the s -channel Z^0 pole. Eq. (24) can in fact hold for the coannihilation corridors, and the minima seen in the mSUGRA models occur here, at essentially the same points as in Fig. 5. However, for the Z^0 bands, μ^2 is quite reduced, and N_{14} is increased violating Eq. (24). Thus no such minima occur for m_0 in the Z^0 bands of Figs. 8 and 9.

IV. D-BRANE MODELS

Recent studies of Type IIB orientifolds have shown that it is possible to construct a number of string models with interesting phenomenological properties [12]. The existence of open string sectors in Type IIB strings implies the presence of Dp-branes, and in the simplest cases, one can consider the full $D = 10$ space compactified on a six torus T^6 . Models of this type contain either 9-branes and 5_i -branes, $i = 1, 2, 3$, or 3-branes and 7_i -branes. Associated with each set of n coincident branes is a gauge group $U(n)$. There are a number of ways in which one can embed the Standard Model in such systems. We consider here the model where $SU(3)_C \times U(1)_Y$ is associated with one set of 5-branes, 5_1 , and $SU(2)_L$ with a second intersecting set 5_2 [11]. Strings starting on 5_1 and ending on 5_2 then carry the joint quantum numbers of the two sets of branes, the massless modes then being the quark and lepton left doublets, and the two Higgs doublets. Strings starting and ending on 5_1 then carry the quantum numbers of that brane, the massless modes being then the quark and lepton right singlets.

Supersymmetry breaking can be treated phenomenologically by assuming that the F components of the dilaton S and the moduli T_i grow VEVs [12,41]:

$$F^S = 2\sqrt{3} \langle \text{Re}S \rangle \sin\theta_b e^{i\alpha_s} m_{3/2} \quad (30)$$

$$F^{T_i} = 2\sqrt{3} \langle \text{Re}T_i \rangle \cos\theta_b \Theta_i e^{i\alpha_i} m_{3/2} \quad (31)$$

where θ_b, Θ_i are Goldstino angles ($\Theta_1^2 + \Theta_2^2 + \Theta_3^2 = 1$). In the following we assume $\Theta_3 = 0$. T-duality determines the Kahler potential [12,41], and using Eqs. (30,31) one generates the soft breaking terms at M_G for the gauginos,

$$\tilde{m}_1 = \tilde{m}_3 = -A_0 = \sqrt{3} \cos\theta_b \Theta_1 e^{-i\alpha_1} m_{3/2} \quad (32)$$

$$\tilde{m}_2 = \sqrt{3} \cos\theta_b (1 - \Theta_1^2)^{1/2} m_{3/2} \quad (33)$$

and for the squarks, sleptons and Higgs,

$$m_{12}^2 = (1 - 3/2 \sin^2 \theta_b) m_{3/2}^2 \quad \text{for } q_L, l_L, H_1, H_2 \quad (34)$$

$$m_1^2 = (1 - 3 \sin^2 \theta_b) m_{3/2}^2 \quad \text{for } u_R, d_R, e_R. \quad (35)$$

Originally this model was considered to examine the possible effects of the new CP violating phases in Eqs.(32,33) and in the μ and B_0 parameters [11,42]. However, it was subsequently seen that unless $\tan\beta$ is small (i.e. $\tan\beta \lesssim 5$) an unreasonable fine tuning of the GUT scale parameters is needed if the experimental constraints on the electron and neutron electric dipole moments are to be obeyed [42]. The LEP data has now eliminated a considerable amount of the low $\tan\beta$ region, and since we are interested here in effects that arise for large $\tan\beta$, we will in the following set all the phases to zero. The model then depends on three parameters: θ_b , Θ_1 , and $m_{3/2}$, with $\theta_b < 0.615$ and $0 < \Theta_1 < 1$, and contains a unique type of nonuniversal soft breaking. In terms of the notation of Eq. (26) one has

$$\delta_1 = \delta_2 = \delta_3 = \delta_7 = -(3/2) \sin^2 \theta_b \quad (36)$$

$$\delta_4 = \delta_5 = \delta_6 = -3 \sin^2 \theta_b \quad (37)$$

where we have equated m_0 to $m_{3/2}$. Note that these nonuniversalities hold for all three generations, not just the third generation. In addition the gaugino masses at M_G are no longer universal (except when $\Theta_1 = 1/\sqrt{2}$), and there are two “effective ” gaugino masses at M_G which we label by $m_{1/2} = \tilde{m}_1 = \tilde{m}_3$, and $m'_{1/2} = \tilde{m}_2$. The A_0 parameter in this model is then fixed by $A_0 = -m_{1/2}$.

We consider first the question of what parts of the parameter space might be accessible to current detectors which obey Eq. (1). From Eqs. (34,35) we see that the sfermion masses decrease with increasing θ_b , and so we expect the largest cross sections to arise for small θ_b , and of course for large $\tan\beta$. However, the $b \rightarrow s\gamma$ constraint eliminates the higher values of θ_b . The limiting boundary obeying Eq. (1) is shown in Fig. 12, where $\sigma_{\tilde{\chi}_1^0-p}$ is plotted for $\tan\beta = 20$ and $\theta_b = 0.2$. For this case, the neutralino mass would be quite small but is still consistent with the LEP bounds¹. (The gap in the middle is due to over annihilation in the early universe through the s-channel Z pole.) The cross section rises, of course with higher $\tan\beta$, and so current detectors are sampling regions where

$$\tan\beta \gtrsim 25 \quad (38)$$

It is easy to see that slepton coannihilation effects exist in this model similar to those of the SUGRA models. Since both the \tilde{e}_R and $\tilde{\chi}_1^0$ both evolve from the GUT scale using the $U(1)$ gaugino, Eq.(16) still holds with m_0^2 replaced $m_{3/2}^2(1 - 3 \sin^2 \theta_b)$. Thus for fixed θ_b , one can adjust $m_{3/2}$ so that the $\tilde{\chi}_1^0$ and \tilde{e}_R are nearly degenerate, allowing for coannihilation to take place. In addition, however, there can be regions of parameter space where there is chargino-neutralino coannihilation. This arises because of the nonuniversal gaugino masses at M_G . Thus from Eqs. (32,33), when Θ_1 gets large, \tilde{m}_2 becomes smaller than \tilde{m}_1 , and the

¹LEP determines the bound on $m_{\tilde{\chi}_1^0}$ by measuring lower bounds on the chargino mass and lower bounds on $m_{\tilde{\chi}_1^0} + m_{\tilde{\chi}_2^0}$ [43]. This combined with lower bounds on the Higgs and slepton masses and the value of the Z width, limits the SUSY parameter space giving rise to the $m_{\tilde{\chi}_1^0}$ bound. Thus the bounds depend on the SUSY model used, and LEP quotes 37 GeV for the MSSM, and 48 GeV for mSUGRA. We have checked that for the D-brane model being considered, the LEP data still implies $m_{\tilde{\chi}_1^0} > 37$ GeV.

$\tilde{\chi}_1^0$ becomes mainly Wino, and can become degenerate with the $\tilde{\chi}_1^\pm$. Coannihilation becomes possible, however, only for a very small range in Θ_1 near 0.9.

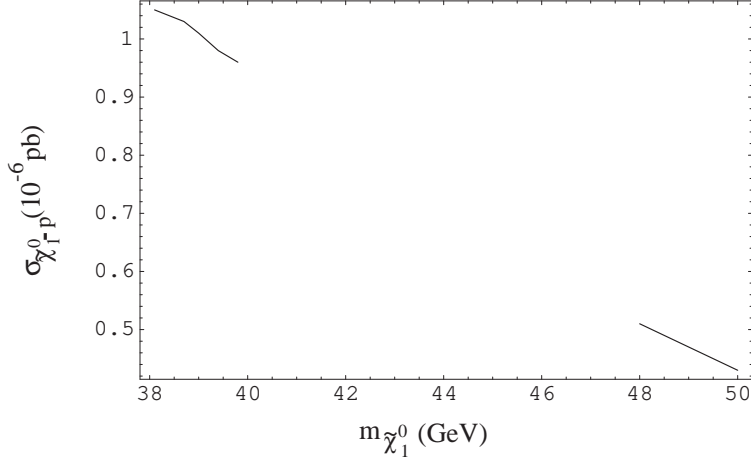


FIG. 12. $\sigma_{\tilde{\chi}_1^0-p}$ for D-brane model for $\mu > 0$, $\theta_b = 0.2$ and $\tan \beta = 20$. The gap in the curve is due to excessive early universe annihilation through the s -channel Z pole.

As in SUGRA models, a cancellation of matrix elements can occur for $\mu < 0$, allowing the cross sections to fall below the sensitivities of planned future detectors. This is exhibited in Fig. 13, where $\sigma_{\tilde{\chi}_1^0-p}$ is plotted for $\tan \beta = 6$ (solid curve), 12 (dot-dash curve), and 20 (dashed curve). (The $\tan \beta = 6$ curve terminates at low $m_{\tilde{\chi}_1^0}$ due to the m_h constraint, while the higher $\tan \beta$ curves terminate at low $m_{\tilde{\chi}_1^0}$ due to the $b \rightarrow s\gamma$ constraint. The upper bound on $m_{\tilde{\chi}_1^0}$, corresponding to $m_{\tilde{g}} < 1$ TeV, arises from the Ωh^2 constraint.) One sees that the cross section goes through a minimum at $\tan \beta \cong 12$, though the expected rise at higher $m_{\tilde{\chi}_1^0}$ does not appear since the parameter space terminates before this sets in.

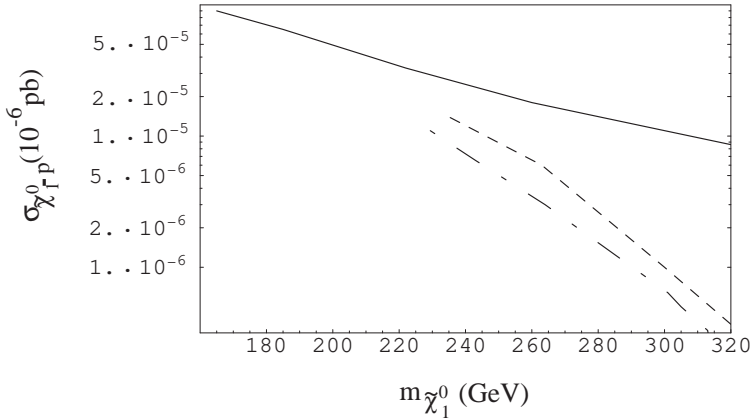


FIG. 13. $\sigma_{\tilde{\chi}_1^0-p}$ for the D-brane model for $\mu < 0$ and $\tan \beta = 6$ (solid), $\tan \beta = 12$ (dot-dash), and $\tan \beta = 15$ (dashed).

V. STOP AND SBOTTOM COANNIHILATION.

It has been known for some time that the nearness of the t -quark Landau pole can significantly lower the \tilde{t}_1 mass [44], and this raises the possibility of $\tilde{t}_1 - \chi$ coannihilation

occurring [45]. Working against this possibility is the positive contributions to $m_{\tilde{t}_1}^2$ from the $SU(3)$ gaugino contribution, and of course the m_t^2 contribution. Nonuniversal soft breaking, however, opens additional possibilities of this type, as it can allow the coefficient of m_0^2 to become negative, reducing further the \tilde{t}_1 mass. To examine this in more detail, we consider the low and intermediate $\tan\beta$ regime where the RGE can be solved analytically. For the \tilde{t}_R one finds

$$\begin{aligned}
m_{\tilde{t}_R}^2 = & \left[D_0 + \left(-\frac{1-D_0}{3}(\delta_2 + \delta_3) + \frac{2+D_0}{3}\delta_4 \right) \right] m_0^2 \\
& + \frac{2}{3} \left[(1-D_0)D_0 \frac{H_3}{F} A_0 m_{1/2} - \frac{1}{2}(1-D_0)D_0 A_0^2 + e m_{1/2}^2 \right] \\
& + \left(\frac{1}{3}f_1 - f_2 + \frac{8}{3}f_3 \right) \frac{\alpha_G}{4\pi} m_{1/2}^2 + m_t^2 + \frac{2}{3} \sin^2 \theta_W M_Z^2 \cos 2\beta
\end{aligned} \tag{39}$$

The f_i form factors, $i = 1, 2, 3$, are numerically approximately 40, 100, 700 respectively, and e , and H_3/F given in [46], are approximately -2 and +2 respectively. One sees that for A_0 large and negative, the Landau pole A_0 terms do give a significant negative contribution and $m_{\tilde{t}_R}^2$ would be minimized for $\delta_{2,3} > 0$ and $\delta_4 < 0$. The universal m_0^2 term, scaled by $D_0 \cong 0.25$, is already quite small, so it does not require too much nonuniversality to achieve a degeneracy with the χ_1^0 . (In fact this can be done even for the universal case if A_0 and $m_{1/2}$ are chosen sufficiently large. However, the degeneracy occurs in that case for parameters in the TeV domain.) Since early universe annihilation cross sections involving the stop are strong interaction phenomena compared with the electroweak neutralino cross sections, the coannihilation effect can be quite significant. However, it is necessary to impose the usual constraints, particularly the $b \rightarrow s\gamma$ bounds, and also that the stop must lie below the stau. Thus a satisfactory coannihilation region occurs only when m_0 is large (e.g. greater than about 800 GeV). The neutralino-proton cross section in this domain generally lies above 10^{-10} pb, and thus should be accessible to future detectors.

Stop coannihilation phenomena are more subtle in the D-brane model, since the nonuniversalities are related i.e. $\delta_2 = \delta_3 = -(3/2) \sin^2 \theta_b m_{3/2}^2 = \delta_4/2$. The m_0^2 term for this case is

$$[D_0 - (1 + 2D_0) \sin^2 \theta_b] m_{3/2}^2 \tag{40}$$

which is negative for $\sin^2 \theta_b \gtrsim 1/6$. (There are also modifications in the gaugino terms to account for their nonuniversal nature in the D-brane model.) Thus stop coannihilation effects can occur also in this model. Here, however, the parameter space for coannihilation is narrowed and generally occurs when $m_{3/2} > 1$ TeV.

b -squark coannihilation phenomena can also occur in these models. For low and intermediate $\tan\beta$, where one may neglect the b -quark Yukawa coupling (relative to the t -quark coupling), the \tilde{b}_R mass is generally large (due to the $SU(3)$ gluino contribution). However, the \tilde{b}_L mass can get small for nonuniversal soft breaking. Thus $m_{\tilde{b}_L}$ is given by

$$\begin{aligned}
m_{\tilde{b}_L}^2 = & \left[\frac{1+D_0}{2} + \left(-\frac{1-D_0}{6}(\delta_2 + \delta_4) + \frac{5+D_0}{6}\delta_3 \right) \right] m_0^2 \\
& + \frac{1}{3} \left[(1-D_0)D_0 \frac{H_3}{F} A_0 m_{1/2} - \frac{1}{2}(1-D_0)D_0 A_0^2 + e m_{1/2}^2 \right] \\
& + \left(-\frac{1}{15}f_1 + f_2 + \frac{8}{3}f_3 \right) \frac{\alpha_G}{4\pi} m_{1/2}^2 + \left(-\frac{1}{2} + \frac{1}{3} \sin^2 \theta_W \right) M_Z^2 \cos 2\beta + m_b^2
\end{aligned} \tag{41}$$

and the light b -squark can be achieved by choosing $\delta_2, \delta_4 > 0$ and $\delta_3 < 0$ so that the coefficient of the m_0^2 term is negative. In this case the light b -squark is mostly \tilde{b}_L , and since the t and b squarks form an $SU(2)$ doublet, the light stop lies just above the light sbottom, and there can be regions where both contribute simultaneously to coannihilation. However, these coannihilation regions again occur for $m_0 > 1$ TeV.

VI. CONCLUSIONS

We have considered in this paper coannihilation effects in dark matter neutralino-proton detection cross sections which arise for large $\tan\beta$ and large values of A_0 for models which have grand unification of the gauge coupling constants at the GUT scale M_G . Coannihilation can occur if the light stau ($\tilde{\tau}_1$), light chargino ($\tilde{\chi}_1^\pm$), light stop (\tilde{t}_1) or light sbottom (\tilde{b}_1) become nearly degenerate with the neutralino. In order to examine these effects for a wide range of models, we have considered SUGRA models with universal soft breaking (mSUGRA), nonuniversal soft breaking in the Higgs and third generation squarks and sleptons, and finally a D-brane model based on type IIB orientifolds which possess nonuniversal gaugino masses. In all these we have imposed the cosmological neutralino relic density constraints as well as accelerator constraints on the SUSY parameter space (including in particular the large $\tan\beta$ NLO corrections to the $b \rightarrow s\gamma$ decay [17,18] as well as the large $\tan\beta$ SUSY corrections to m_b and m_τ). Radiative breaking of $SU(2) \times U(1)$ at the electroweak scale also gives strong constraints on the theory.

mSUGRA illustrates some of the effects arising for large $\tan\beta$. Thus for low $\tan\beta$, the regions in the $m_0 - m_{1/2}$ plane allowed by the relic density constraint Eq. (4) is relatively insensitive to A_0 . However, for large $\tan\beta$, the $b \rightarrow s\gamma$ constraint allows only the $\tilde{\tau}_1 - \tilde{\chi}_1^0$ coannihilation corridors to remain (except for some small islands when $m_{1/2} \lesssim 350$ GeV) and as A_0 increases, these corridors have increasing m_0 . Thus m_0 can rise to 1 TeV for large $m_{1/2}$. (See e.g. Fig. 1.) This lowers the value of $\sigma_{\tilde{\chi}_1^0-p}$ and even though $\sigma_{\tilde{\chi}_1^0-p}$ increases rapidly with $\tan\beta$, the value of $\sigma_{\tilde{\chi}_1^0-p}$ at large $\tan\beta$ and large A_0 can be smaller than $\sigma_{\tilde{\chi}_1^0-p}$ at $\tan\beta = 3$, as illustrated in Fig.4. For $\mu > 0$, however, one generally finds for the parameter space of Eqs. (6-8) that $\sigma_{\tilde{\chi}_1^0-p} \gtrsim 10^{-10}$ pb, and so should be accessible to future detectors. In the high $\tan\beta$ domain, the $b \rightarrow s\gamma$ constraint produces a lower bound on $m_{1/2}$, which decreases with increasing A_0 . Thus one finds that $m_{\tilde{\chi}_1^0} \gtrsim 120$ GeV ($m_{\tilde{g}} \gtrsim 740$ GeV) for $A_0 = 4m_{1/2}$, $\tan\beta = 40$, $\mu > 0$.

For $\mu < 0$, a special cancellation can occur in mSUGRA allowing $\sigma_{\tilde{\chi}_1^0-p}$ to become much less than 10^{-10} pb, as has been previously noted for low and intermediate $\tan\beta$ [31]. The analytic origin of this effect is discussed in Sec. 2. The effect, however, occurs only for a fixed range of $\tan\beta$. Thus the position of these minima begins for $\tan\beta \cong 7$ at $m_{1/2} = 1000$ GeV, moves to lower $m_{1/2}$ until $\tan\beta$ increases to 10, and then increases to beyond $m_{1/2} = 1000$ GeV at $\tan\beta \gtrsim 30$. (See Fig. 5.) We note that while the cancellation occurs at a fixed value of $m_{1/2}$, the effects spread over a wide range of $m_{1/2}$ and in this region, halo dark matter would be inaccessible to current or planned detectors. However, if the recently reported anomaly in the muon gyromagnetic ratio [47] is indeed due to supersymmetry, then μ is positive and this case would be eliminated.

The nonuniversal soft breaking models illustrate new phenomena at large $\tan\beta$ not

present in mSUGRA, and one can also understand these effects analytically. Thus the value of μ^2 , obtained from radiative breaking of $SU(2) \times U(1)$, is a major element in controlling the value of $\sigma_{\tilde{\chi}_1^0-p}$, and lowering μ^2 increases $\sigma_{\tilde{\chi}_1^0-p}$. Thus for one sign of the nonuniversalities, $\sigma_{\tilde{\chi}_1^0-p}$ can be increased by a factor of 10 or more, allowing current detectors to sample the parameter space with $\tan \beta$ as low as $\cong 7$. (See Fig. 7.) For large $\tan \beta$ a new effect can occur. The value of μ^2 also controls the gaugino/higgsino content of the $\tilde{\chi}_1^0$, and lowering μ^2 increases the amount of Higgsino in the $\tilde{\chi}_1^0$. This then increases the amount of early universe annihilation via an off shell s-channel Z boson, which opens an additional allowed region in the $m_0 - m_{1/2}$ plane, considerably wider than the $\tilde{\tau}_1$ coannihilation corridor and at much higher m_0 . (See Fig. 8.) (Other simple choices of nonuniversal parameters can also raise the values of m_0 for the $\tilde{\tau}_1$ coannihilation corridor, as illustrated in Fig.9.) Though m_0 is large for this Z -channel annihilation, reducing $\sigma_{\tilde{\chi}_1^0-p}$, this effect is compensated by the fact that μ^2 is decreased (which raises $\sigma_{\tilde{\chi}_1^0-p}$). Thus $\sigma_{\tilde{\chi}_1^0-p}$ remains relatively large (see Figs. 10, 11), and this region of parameter space should become experimentally accessible in the relatively near future (e.g. when CDMS moves to the Soudan mine).

The D-brane model examined is quite constrained as all the squark and slepton nonuniversalities are controlled by a single parameter θ_b . Current detectors are sampling parts of the parameter space where $\tan \beta \gtrsim 25$. Because these models have also nonuniversal gaugino masses, the LEP lower bound on $m_{\tilde{\chi}_1^0}$ is much smaller than in SUGRA models, i.e. the same as in the MSSM: $m_{\tilde{\chi}_1^0} \geq 37$ GeV. However, the gaugino nonuniversality still allows the usual type of $\tilde{\tau}_1 - \tilde{\chi}_1^0$ coannihilation to occur. A unique feature of the gaugino nonuniversality is that \tilde{m}_2 can become smaller than \tilde{m}_1 allowing the $\tilde{\chi}_1^0$ to become mostly Wino and a $\tilde{\chi}_1^\pm - \tilde{\chi}_1^0$ coannihilation domain to exist. However, the near degeneracy of $\tilde{\chi}_1^\pm$ and $\tilde{\chi}_1^0$ occurs only for a very small region of parameter space (when $\Theta_1 \cong 0.9$). The cancellation phenomena in $\sigma_{\tilde{\chi}_1^0-p}$ for $\mu < 0$ also occurs for these D-brane models, the minimum value of $m_{\tilde{\chi}_1^0}$ where the cancellation is complete occurring at $m_{\tilde{\chi}_1^0} \cong 315$ GeV for $\tan \beta \cong 12$.

Nonuniversal SUGRA models also allow for $\tilde{t}_1 - \tilde{\chi}_1^0$ coannihilation to occur. In this case, the light stop is mostly \tilde{t}_R . Then for $A_0 < 0$, the Landau pole contributions to $m_{\tilde{t}_R}^2$ are negative, and one can chose nonuniversal soft breaking so that the coefficient of m_0^2 is also negative. The \tilde{t}_1 then becomes nearly degenerate with the $\tilde{\chi}_1^0$ when $m_0 \gtrsim 800$ GeV, coannihilation setting in for that domain. Actually, $\tilde{t}_1 - \tilde{\chi}_1^0$ can also occur in mSUGRA, but to achieve the near degeneracy one needs $A_0 > 4m_{1/2}$. Similarly, this coannihilation can occur for the D-brane model but for $m_{3/2} > 1$ TeV.

In a similar fashion, $\tilde{b}_1 - \tilde{\chi}_1^0$ coannihilation can occur for nonuniversal models when the \tilde{b}_1 is mainly \tilde{b}_L . Thus one may chose $A_0 < 0$ and nonuniversal parameters in $m_{\tilde{b}_L}^2$ so that the coefficient of m_0^2 is negative, making the \tilde{b}_1 nearly degenerate with the $\tilde{\chi}_1^0$. This coannihilation only sets in, however, for $m_0 > 1$ TeV.

VII. ACKNOWLEDGEMENT

This work was supported in part by National Science Foundation grant No. PHY-0070964.

Note added: After completing this paper there appeared the paper “The CMSSM Parameter

Space at Large $\tan\beta$ " by J. Ellis, T. Falk, G. Gani, K.A. Olive and M. Srednicki, hep-ph/0102098. This paper considers large $\tan\beta$ effects for the mSUGRA model only, and is restricted to $A_0 = 0$.

REFERENCES

- [1] G. Jungman, M. Kamionkowski and K. Griest, *Phys. Rep.* **267**, 195 (1995); E. Kolb and M. Turner, *The Early Universe*, Addison-Wesley, Reading, 1990.
- [2] K. Griest and D. Seckel, *Phys. Rev. D* **43**, 3191 (1991).
- [3] P. Gondolo and G. Gelmini, *Nucl. Phys. B* **360**, 145 (1991).
- [4] R. Arnowitt and P. Nath, *Phys. Lett. B* **299**, 58 (1993); *Phys. Lett. B* **303**, 403 (1993) (Erratum).
- [5] J. Edsjo and P. Gondolo, *Phys. Rev. D* **56**, 1879 (1997).
- [6] J. Ellis, T. Falk and K.A. Olive, *Phys. Lett. B* **444**, 367 (1998).
- [7] J. Ellis, T. Falk, K.A. Olive and M. Srednicki, *Astropart. Phys.* **13**, 181 (2000).
- [8] For previous works see e.g. M.E. Gomez, G. Lazarides and C. Pallis, *Phys. Rev. D* **61**, 123512 (2000); *Phys. Lett. B* **487**, 313 (2000); S. Khalil, G. Lazarides and C. Pallis, hep-ph/0005021; M.E. Gomez and J.D. Vergados, hep-ph/0012020.
- [9] A.H. Chamseddine, R. Arnowitt and P. Nath, *Phys. Rev. Lett.* **49**, 970 (1982); R. Barbieri, S. Ferrara and C.A. Savoy, *Phys. Lett. B* **119**, 343 (1982); L. Hall, J. Lykken and S. Weinberg, *Phys. Rev. D* **27**, 2359 (1983); P. Nath, R. Arnowitt and A.H. Chamseddine, *Nucl. Phys. B* **227**, 121 (1983).
- [10] V. Berezhinsky, A. Bottino, J. Ellis, N. Fornengo, G. Mignola and S. Scopel, *Astropart. Phys.* **5**, 1 (1996); *Astropart. Phys.* **6**, 333 (1996); P. Nath and R. Arnowitt, *Phys. Rev. D* **56**, 2820 (1997); R. Arnowitt and P. Nath, *Phys. Lett. B* **437**, 344 (1998); A. Bottino, F. Donato, N. Fornengo and S. Scopel, *Phys. Rev. D* **59**, 095004 (1999); R. Arnowitt and P. Nath, *Phys. Rev. D* **60**, 044002 (1999).
- [11] M. Brhlik, L. Everett, G. Kane and J. Lykken, *Phys. Rev. D* **62**, 035005 (2000).
- [12] L. Ibanez, C. Munoz and S. Rigolin, *Nucl. Phys. B* **536**, 29 (1998).
- [13] G. Jungman et al., in Ref. 1.
- [14] A. Bottino and N. Fornengo, hep-ph/9904469
- [15] A. Corsetti and P. Nath, *Int. J. Mod. Phys. A* **15**, 905 (2000).
- [16] P. Igo-Kimenes, talk presented at ICHEP 2000, Osaka, Japan, July 27 - August 2, 2000.
- [17] G. Degrassi, P. Gambino and G. Giudice, *JHEP* **0012**, 009 (2000).
- [18] M. Carena, D. Garcia, U. Nierste and C. Wagner, hep-ph/0010003.
- [19] I. Trigger, OPAL Collaboration, talk presented at DPF 2000, Columbus, OH; T. Alderweireld, DELPHI Collaboration, talk presented at DPF 2000, Columbus, OH.
- [20] D0 Collaboration, *Phys. Rev. Lett.* **83**, 4937 (1999).
- [21] M. Alam et al., *Phys. Rev. Lett.* **74**, 2885 (1995).
- [22] M. Fukugita, hep-ph/0012214.
- [23] J. Ellis and R. Flores, *Phys. Lett. B* **263**, 259 (1991); *Phys. Lett. B* **300**, 175 (1993).
- [24] A. Bottino, F. Donato, N. Fornengo and S. Scopel; *Astropart. Phys.* **13**, 215 (2000).
- [25] H. Leutwyler, *Phys. Lett. B* **374**, 163 (1996).
- [26] M. Olsson, *Phys. Lett. B* **482**, 50 (2000); M. Pavan, R. Arndt, I. Strakovsky and R. Workman, nucl-th/9912034.
- [27] J. Gasser and M. Sainio, hep-ph/0002283.
- [28] R. Arnowitt, B. Dutta and Y. Santoso, hep-ph/0010244, hep-ph/0101020.
- [29] A. Bottino et al., in ref. [9].
- [30] J. Ellis, T. Falk, K.A. Olive and M. Srednicki, *Astropart. Phys.* **13**, 181 (2000).
- [31] J. Ellis, A. Ferstl and K.A. Olive, *Phys. Lett. B* **481**, 304 (2000).

- [32] J. Ellis, T. Falk, G. Ganis and K.A. Olive, *Phys. Rev. D* **62**, 075010 (2000).
- [33] E. Accomando, R. Arnowitt, B. Dutta and Y. Santoso, *Nucl. Phys. B* **585**, 124 (2000).
- [34] R. Arnowitt, B. Dutta and Y. Santoso, hep-ph/0005154.
- [35] M. Srednicki, R. Watkins and K.A. Olive, *Nucl. Phys. B* **310**, 693 (1988).
- [36] L. Ibanez and C. Lopez, *Nucl. Phys. B* **233**, 511 (1984).
- [37] J. Gunion, H. Haber, G. Kane and S. Dawson, *The Higgs Hunter's Guide*, Addison-Wesley, Reading, 1990.
- [38] V. Bednyakov and H. Klapdor-Kleingrothaus, hep-ph/0011233.
- [39] P. Nath and R. Arnowitt, *Phys. Rev. D* **56**, 2820 (1997).
- [40] J. Ellis, A. Ferstl and K. Olive, hep-ph/0007113.
- [41] A. Brignole, L. Ibanez, C. Munoz and C. Scheich, *Z. Phys. C* **74**, 157 (1997); A. Brignole, L. Ibanez and C. Munoz, *Nucl. Phys. B* **422**, 125 (1994); Erratum *ibid.* **B436**, 747 (1995).
- [42] E. Accomando, R. Arnowitt, B. Dutta, *Phys. Rev. D* **61**, 075010 (2000).
- [43] ALEPH collaboration, CERN EP/2000-139.
- [44] P. Nath, J. Wu and R. Arnowitt, *Phys. Rev. D* **52**, 4169 (1995); M. Carena and C.E.M. Wagner, *Nucl. Phys. B* **452**, 45 (1995).
- [45] For earlier work see C. Boehm, A. Djouadi and M. Drees, *Phys. Rev. D* **62**, 035012 (2000).
- [46] L. Ibanez, C. Lopez, C. Munoz, *Nucl. Phys. B* **256**, 218 (1985).
- [47] H.N. Brown et.al., hep-ex/0102017.